Blends of Reverse Enteric Polymer with Enteric and pH-Independent Polymers: Mechanistic Investigations for Tailoring Drug Release

Anupa R. Menjoge and Mohan G. Kulkarni*

Polymer Science and Engineering Division, National Chemical Laboratory, Pune 411008, India

Received June 6, 2006; Revised Manuscript Received October 24, 2006

Blends of conventional reverse enteric polymer with enteric polymers result in insoluble polyelectrolyte complexes and hence cannot be used in film coatings. We report a new set of miscible blends of a new reverse enteric polymer (NREP) synthesized by us with enteric and pH-independent polymers. The nature of interactions between polymers in the blends has been established by analyzing Fourier transform infrared (FTIR) spectra. The extent of interaction has been investigated by thermal analysis and quantified in terms of parameters K_1 and K_2 in the Schneider equation. Based on these values, the interactions between NREP and these polymers have been ranked in the order EC (ethylcellulose) < ES (Eudragit S) < HPMCP (hydroxypropyl methylcellulose phthalate). The quantification of interactions in blends helps explain the release pattern of cefuroxime axetil (CA) at gastric pH and tailor the release of other drugs according to their pharmacokinetic characteristics. The understanding also provides a more rational approach for selection of polymers and their content in the coating compositions, rather than an empirical approach.

Introduction

Polymer blends are extensively used in controlled drug delivery systems as they enable tailoring drug release profiles in ways not possible with individual polymers.[1,2] However, existing polymers and their blends have not been very useful in achieving sustained release of cefuroxime axetil (CA) without sacrificing palatability and bioavailability. CA, a second-generation cephalosporin antibiotic administered orally, has a short half-life of 2 h.[3] It has a limited absorption window restricted to upper gastric region. Oral bioavailability of CA is 37−52%.[3] Intestinal enzyme esterase hydrolyzes CA to cefuroxime, a form not absorbed orally.[4−6] Hence enteric coating polymers, that is, polyacids that release the drug in the intestinal region, would further lower CA bioavailability. It is therefore essential to release CA in the gastric region (acidic pH) so that its bioavailability is not further affected. Extensive efforts have been made in the past to coat CA by use of cellulose acetate trimellitate (CAT), hydroxypropyl methylcellulose phthalate (HPMCP), and Eudragit E (EE).[7,8] CA was completely degraded in the presence of EE and led to unacceptably high proportions of impurities in the presence of CAT.[7,8]

The slow permeation of moisture from film coat into the tablet core results in gelation of CA, leading to poor dissolution and reduced absorption.[9] Apart from these, CA is extremely bitter in taste and a barrier coating to mask its taste is essential.[10] Delayed-release systems will not be effective for CA due to its restricted absorption region, and gastroretentive systems like floating tablets are difficult to formulate due to gelling tendency. The rational design of a sustained-release delivery system for CA needs to take into account the trinity of *drug*, *delivery*, and *destination.* The physicochemical and pharmacokinetic characteristics of CA have restricted the formulation development using commercially available polymers. This has educed the need to develop a polymer capable of catering to these needs.

To overcome the above limitations, we undertook the development of a new reverse enteric polymer (NREP), which dissolves at gastric pH and is useful for the development of taste-masked, immediate, and sustained gastric release delivery systems.[11] Evaluation of the biological reactivity (in vitro and in vivo) was undertaken to ensure biocompatibility. A detailed investigation of physicochemical interactions between CA and NREP by differential scanning calorimetry (DSC), Fourier transform infrared (FTIR), NMR spectroscopy, and HPLC analysis was undertaken. The self-associations within NREP and its lower basicity prevent the interaction between NREP and CA. We evaluated the blends of NREP with other polymers to bring about sustained release at gastric pH.[11]

The literature reveals numerous investigations on phase behavior of polymer blends.[12−14] However, there are no reports describing systematic investigations on the extent of interactions within the polymer blend responsible for blend miscibility and correlating it with the drug release. The present investigation reports a new set of film-forming polymer blends containing reverse enteric and enteric polymers for tailoring drug release. The nature of interactions between the constituents of polymer blends has been established by analyzing FTIR spectra. The extent of interactions has been investigated by thermal analysis and quantified in terms of parameters K_1 and K_2 in the Schneider equation. On the basis of these values, the interactions between NREP and Zein, EC, ES, and HPMCP have been ranked in the order EC < ES < HPMCP. These investigations help interpret the drug release pattern from the blends, based on the extent of interactions between blend constituents. The results of the mechanistic investigations provide a more rational approach to tailor polymer blends for drug release. The utility of the blends in sustained release of CA under gastric conditions has been established. CA encapsulated in these polymer blends can be formulated as solid dosage forms and also as liquid oral formulations.[15]

* Corresponding author: tel +91-20-25902178; fax + 91-20-25902618; e-mail mg.kulkarni@ncl.res.in.

10.1021/bm060540+ CCC: $37.00
Published on Web 12/05/2006

Table 1. NREP Characteristics

	composition (%)				
	feed	by NMR	MW[a]	PI[b]	T_g (°C)
MMA	60	62			
HEMA	25	27	58 550	1.6	121.2
VP	15	11			

[a] MW, molecular weight. [b] PI, polydispersity index.

Experimental Section

Materials. Eudragit S 100 (ES) (Degussa/Rohm Pharma), hydroxypropyl methylcellulose phthalate (HPMCP) (Eastman), ethylcellulose (EC), and cefuroxime axetil were gifts from Lupin Laboratories Ltd, India. Zein, methyl methacrylate (MMA), 2-hydroxyethyl methacrylate (HEMA), and 4-vinylpyridine were purchased from Sigma−Aldrich. The solvents methanol (MeOH), dichloromethane (DCM), and chloroform ($CHCl_3$) were purchased from Qualigens. Dimethylformamide (DMF) was purchased from Merck. Azobis(isobutyronitrile) (AIBN) was purchased from a local supplier.

Synthesis of New Reverse Enteric Polymer. NREP was synthesized as disclosed by us earlier.[16,17] The trace impurity of EGDMA (ethylene glycol dimethacrylate) was removed from HEMA before polymerization to yield soluble polymer. Freshly distilled monomers MMA and 4VP were used for polymerization. In a 250 mL round-bottom flask, 18.72 g of MMA (0.186 mol), 11.58 g of HEMA (0.088 mol), and 5.07 g of 4-VP (0.048 mol) were added to 80 mL of DMF. Solution polymerization of the monomer mixture was carried out with 0.35 g of AIBN (0.002 mol) as initiator at 65 °C for 18 h. The polymer solution was concentrated on a rotaevaporator. The polymer was dissolved in (1:1 v/v) DCM−MeOH mixture and precipitated in water to remove unreacted monomers. Polymer was dried at 27 °C under vacuum for 72 h. The polymer composition is given in Table 1 and the structure is shown in Scheme 1.

Preparation of Polymer Blends. The blends of ES, HPMCP, EC, and Zein with NREP were prepared by solution casting method from a mixture of MeOH−$CHCl_3$ (20:80). Films of NREP and above polymers were prepared in the weight ratio 25:75, 34:66, 50:50, 66:34, and 75:25 (% w/w).

Physicochemical Characterization of Polymer Blends: FTIR Spectroscopy. The interactions between NREP and ES, EC, HPMCP, and Zein were examined by FTIR spectroscopy on a Perkin-Elmer Spectrum One instrument in diffuse reflectance mode. Sample (2−3 mg) was thoroughly mixed, triturated with potassium bromide (100 mg), placed in the sample holder, and scanned from 4000 to 450 cm^{-1}. The measuring conditions were 4.0 resolution, 2.0 zero-fitting, 16 sample scans, and single-sided acquisition. The peaks were marked by use of the Perkin-Elmer spectroscopy software by peak picking at suitable thresholds. The peak assignments for neat polymers were compared with the peaks obtained for the polymer blends (50:50 w/w %). The peak assignments for the neat polymers are as follows (see structures of polymers in Scheme 1S, Supporting Information);

NREP. IR (KBr, cm^{-1}) 3541 (OH, free OH groups); 1726 (C═O, ester), 2839−2992 (methyl C−H asym/sym stretch); 1448−1482 (methyl C−H asym/sym bend); 1190−1270 (C−O stretch); 1558−1601, 990 (characteristic for pyridine ring).

Scheme 1. Structure of NREP

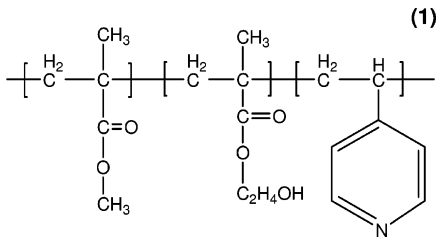

ZEIN. IR (KBr, cm^{-1}) 1660 (amide I, C═O stretching vibrations); 1530 (amide II, N−H bending vibration). Duodu et al.[18] described similar assignments.

EC. IR (KBr, cm^{-1}) 3485 (broadband for OH groups); 2976, 2878 (methyl C−H asym/sym stretch); 1448, 1486 (methylene C−H bend); 1375 (C−H bending); 1131, 1064 (cyclic ether C−O stretch in C−O−C). These assignments are similar to those described in the past.[19,20]

ES. IR (KBr, cm^{-1}) 2500−3500 (OH groups); 2950−2997 (methyl C−H asym/sym stretch); 2839 [methoxy (CH_3−O−), C−H stretch]; 1728 (esterified carboxylic acid, C═O); 1388, 1449, 1484 (methyl C−H vibrations, asym/sym stretch); 1150, 1193, 1270 (ester vibrations). These values are similar to those assigned by Cilurzo et al.[21]

HPMCP. IR (KBr, cm^{-1}) 3460 (O−H groups); 2989, 2884 (methyl C−H asym/sym stretch); 2938 (methylene C−H asym/sym stretch); 2828 (methoxy O−CH_3), 1725 (C═O, ester); 1599 (C═C conjugated vinyl, aromatic ring); 1448, 1486 (methylene C−H bend); 1285 (ester bond C−O−C); 1128, 1067 (cyclic ether C−O stretch in C−O−C); 949 (aromatic C−H in plane bend), 746 (monosubstituted aromatic ring). Similar assignments were reported in the past.[19]

DSC Analysis. Neat polymers and the blends were subjected to thermal analysis on a TA Instruments DSC Q100 V9.0 built 275, by the modulated differential scanning calorimetry (MDSC) heat-only method, with nitrogen as purge gas (flow rate of 50 mL/min). The modulation amplitude was ±0.53 °C every 40 s. Indium was used to calibrate the enthalpy and temperature values. The experiments were conducted in crimped sealed aluminum pans, and 1−2 mg of sample was scanned from 10 to 200 °C at 5 °C/min.

Determination of CA Content. CA content was determined by dissolving 50 mg of microparticles in 2 mL of MeOH and sonicating for 5 min. The volume was made to 50 mL with 0.07 N HCl. The solution was filtered and diluted further for analysis. The absorbance of solution was measured at 278 nm on a Shimadzu UV160 IPC UV−visible spectrophotometer. Each sample was analyzed in triplicate.

CA Release Studies. Microparticles containing cefuroxime equivalent to 125 mg were placed in a basket of 900 mL of 0.07 N HCl. The dissolution was carried out in Electrolab USP type II apparatus at 75 rpm at 37 ± 0.5 °C. The samples were collected after 30, 60, 90, 120, 180, and 240 min while the sink condition was maintained. The dissolution tests were done in triplicate.

Scanning Electron Microscopy. Leica UK model Stereoscan 400 was used to scan the morphological changes in microparticles after dissolution. The samples were gold-sputtered before scanning.

Encapsulation of CA by Use of Polymer Blends. CA was encapsulated by an emulsification solvent evaporation method. NREP−polymer blend solutions were prepared in mixture of MeOH−DCM (1:1 v/v). CA was added to polymer blend solution under magnetic stirring. The CA−polymer solution was dispersed slowly in light liquid paraffin containing 0.25% Span 85 under mechanical stirring. The stirring was continued for 3−4 h at 500 rpm. The microparticles were separated by filtration, washed with petroleum ether to remove the paraffin oil, and dried under vacuum for 24 h at room temperature.

Drug Release from Miscible Polymer Blends: Theoretical Considerations. Miscibility of Polymers. Polymer blends in general are immiscible, since entropy of mixing is small and does not compensate for unfavorable endothermic heat of mixing. Miscibility is achieved by incorporating functional groups in either or both components of the blends. The interactions between functional groups, which could be electrostatic, dipole−dipole resonance, proton transfer, and hydrogen bonding, result in exothermic mixing, leading to miscibility. On the basis of the extent of interaction, the blends are categorized as immiscible, partially miscible, and miscible. Release of drug from polymer blends depends on the extent of these interactions.

Miscibility of a wide range of polymers has been investigated by a variety of techniques such as DSC, microscopy, light scattering, inverse gas chromatography, rheology, and spectroscopy.[12−14] The estimation of glass transition temperature (T_g) is the tool most widely used to evaluate polymer blend miscibility. The immiscible blends exhibit two

T_gs corresponding to the individual polymers. In partially miscible blends, the two T_g values shift depending upon extent of miscibility. At the other extreme, when the interactions between the blend components are strong, interpolymer complexes are formed that exhibit T_g values higher than individual polymers in blend. The blend miscibility resulting from weak interactions between the polymers results in T_g intermediate to the values for individual polymers.

The Fox equation, which assumes volume additivity of mixing, provides the simplest frame work to correlate T_gs of blends.[22] According to eq 1

$$\frac{1}{T_g} = \frac{X_1}{T_{g1}} + \frac{X_2}{T_{g2}} \quad (1)$$

where T_{g1} and T_{g2} represent T_gs of polymers 1 and 2, and X_1 and X_2 are weight fractions of polymers 1 and 2. The T_gs of polymer blends may exhibit both positive and negative deviations from composition dependence predicted by eq 1. Further, the deviations are often not monotonous. A large number of approaches to correlate composition dependence of T_g of blends have been proposed and have been reviewed by Schneider.[22,23] We have chosen to analyze the composition dependence of T_gs of blends in the framework of the Schneider equation[24] as it accounts for both positive and negative deviations from eq 1 as well as the sigmoidal T_g versus composition curves. The miscible polymer blends result from homo- and heteromolecular contacts between the binary blend components. The number of each type of contact will depend upon the volume fraction of each component. Each of these contacts will make a different contribution to the T_g of blends.

In development of correlation for T_g of blends, Brekner et al.[25] considered the parameter K_1 to account for the deviations from additivity due to the difference between contributions of hetero- and homomolecular contacts to the T_g of the blend. Furthermore, these contacts also influence the free volume distribution in the vicinity of the contact. The effect of this redistribution on T_g determines the magnitude of the parameter K_2. Since this redistribution also influences the formation of contacts, the parameter K_1 depends on both the contribution of hetero contacts to T_g and the influence of changes in free volume in the neighborhood on the contribution of contacts. Considering the effect of these two factors on the deviations from volume additivity, and application of appropriate boundary conditions, the following equation was arrived at to correlate the dependence of T_g on the blend composition:

$$(T_g - T_{g1})/(T_{g2} - T_{g1}) = (1 + K_1)\phi - (K_1 + K_2)\phi^2 + K_2\phi^3 \quad (2)$$

where K_1 is related to the difference in interaction energies of hetero and homo contacts in polymer blend, K_2 accounts for the energetic perturbations in molecular surrounding of the hetero contacts in blend, and ϕ represents the volume fraction of the component with high T_g. The condition $K_2 = 0$ assumes effects of molecular surroundings for all contacts to be identical. However, $K_1 = 0$ necessitates that $K_2 = 0$, which then leads to volume additivity. Equation 2, when converted to the corrected weight fraction (W_{2c}) of the component having higher T_g, results in

$$(T_g - T_{g1})/(T_{g2} - T_{g1}) = (1 + K_1)W_{2c} - K_1 + K_2W_{2c}^2 + K_2W_{2c}^3 \quad (3)$$

where $W_{2c} = [K'(T_{g1}/T_{g2})w_2]/[w_1 + K'(T_{g1}/T_{g2})w_2]$ and w_1 and w_2 are weight fractions of components 1 and 2 in blend, respectively. However, in most cases both positive and negative deviations from volume additivity are observed.[24] In some cases sigmoidal plots for T_g versus composition curves are obtained. These deviations are best quantified by estimating fitting parameters K_1 and K_2. The term $(K_1 - K_2)$ is a measure of deviations in T_g observed as a result of differences between the contributions from hetero- and homomolecular contacts to the T_g of the blend.

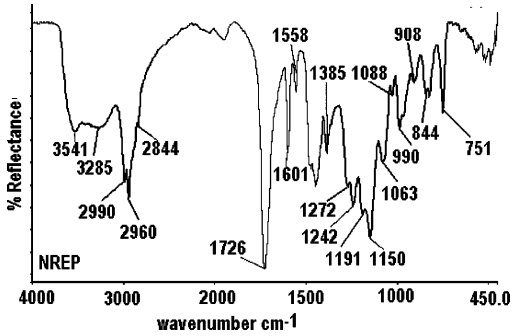

Figure 1. FTIR spectrum of NREP.

Mathematical Model for Release from Blends. The release data were treated with the general equation put forth by Ritger and Peppas[26] for nonswellable devices:

$$M_t/M_\infty = kt^n \quad (4)$$

where M_t/M_∞ is the fraction of drug released at time t, k is the proportionality constant that accounts for the structural and geometrical properties of the matrix, and n is the diffusional exponent indicative of the drug release mechanism. Equation 4 adequately describes the release of drugs from slabs, spheres, cylinders and tablets. In the case of Fickian release, the exponent n has a limiting value of 0.50, 0.45, and 0.43 from slabs, cylinders, and spheres, respectively. The values of n and k are inversely related, and a higher value of k suggests a burst release of drug from the matrix.[27]

Results and Discussion

FTIR Spectroscopy. Infrared spectroscopy is extensively used in the analysis of polymer blends.[28] Among various types of associations that render polymer blends miscible, hydrogen bonding is the most common.[29] Hydrogen bonding affects absorption bands in the region 3500−3600 cm^{-1}. The other regions affected by polymer miscibility include C═O stretching (1734 cm^{-1}), $-CH_2$ symmetric stretching (2886 cm^{-1}), and the fingerprint region (1300−650 cm^{-1}).[30] Strong interactions between polyacids and polybases result in polyelectrolyte complexes, and a new band for carboxylate salt is seen between 1500 and 1600 cm^{-1}.[31,32] In the present study this technique is used to correlate the effect of interactions between the polymers, their miscibility, and effect on drug release. It was observed that as the extent of interaction increased; the protonation of NREP is suppressed, which in turn affects the release pattern.

FTIR Spectra of NREP. NREP is a terpolymer comprising MMA, HEMA, and 4VP. It contains both proton-accepting and -donating groups. The carbonyl groups from MMA and HEMA act as proton acceptors and are capable of interacting with the proton-donating groups. The pyridine nitrogen is a proton acceptor and is capable of forming hydrogen bonds. The hydroxyl group of HEMA is a proton-donating group. It is expected that NREP should exhibit self-association by hydrogen bonding between hydroxyl−carbonyl or hydroxyl−hydroxyl and hydroxyl−pyridine nitrogen (see Scheme 2S in Supporting Information and Figure 1).

Hydroxyl Stretching Region (3100−3650 cm^{-1}). The bands at 3285 and 3541 cm^{-1} arise from several contributions corresponding to hydroxyl groups in different environments. The band at 3285 cm^{-1} in NREP corresponds to hydrogen-bonded hydroxyl of HEMA co-monomer. This band shows a shoulder at 3541 cm^{-1} corresponding to free hydroxyl group. The maximum at 3285 cm^{-1} represents intramolecular associated hydroxyl groups in NREP. Similar bands for hydrogen-bonded

hydroxyl groups were observed in poly(HEMA).[33] The subsequent section discusses the associations of hydroxyl groups from HEMA with carbonyl and pyridine nitrogen from co-monomers MMA and 4VP in NREP.

Carbonyl Stretching Region (1650−1740 cm^{-1}). The spectrum of poly(MMA) shows a band at 1730 cm^{-1} for carbonyl groups.[34] The band at 1726 cm^{-1} in NREP corresponds to carbonyl of MMA and HEMA. In addition, a shoulder is seen at 1636 cm^{-1}, indicating self-association within NREP arising from intramolecular hydrogen bonding between carbonyl and hydroxyl groups. Hydrogen bonding between carbonyl and hydroxyl within poly(HEMA) and carbonyl of poly(MMA) with free hydroxyl groups of celluosic polymer has been reported in the past.[33,35] This substantiates our findings.

Pyridine Ring Mode (1540−1640 cm^{-1}). The most intense bands for pyridine ring are located at 1558, 1597, and 990 cm^{-1}.[33,36] In poly(4-VP) the band at 1558 cm^{-1} is unaffected by hydrogen bonding of nitrogen, whereas the bands at 1597 and 990 cm^{-1} show a shift. In the copolymer HEMA-*co*-4VP, the preference of hydroxyl groups over carbonyl for interaction with pyridine nitrogen has been reported.[33] NREP shows bands for pyridine at 1601, 1558, and 990 cm^{-1}. In the past, a shift from 1597 to 1603 cm^{-1} for hydrogen-bonded pyridine was reported.[36,37] In NREP a shift from 1597 to 1601 cm^{-1} for the pyridine band is seen, indicating hydrogen bonding between pyridine nitrogen and hydroxyls from HEMA.

Potential Interactions with NREP. Poly(4VP) is reported to undergo hydrogen bonding (pyridine nitrogen acts as proton acceptor), coordination complexation (lone electron pair of nitrogen) and charge-transfer (acid/base interactions).[38] 4VP imparts basic character to NREP. Hence NREP should be capable of forming hydrogen bonds with polyacids. Strong interactions between polyacids and polybases involve proton transfer, leading to salt formation.[39] The chemical structure of NREP indicates that the free hydroxyl from HEMA and carbonyl from HEMA as well as MMA and pyridine nitrogen can contribute toward hydrogen bonding. Also it was of interest to investigate whether intramolecular association in NREP would be overcome by intermolecular associations in its blends with Zein, EC, ES, and HPMCP.

A comprehensive analysis of hydroxyl and carbonyl stretching regions and the pyridine ring modes was undertaken. Of special significance was the pyridine ring mode, as it differentiates between strong and weak interactions. Complexation of pyridine to metal ions and sulfonic acid has been reported.[38,40−41] The complexation of pyridine involves proton transfer with conversion to pyridinium. Protonation of pyridine results in the appearance of new band between 1618 and 1637 cm^{-1} and the disappearance of bands at 1597 and 1558 cm^{-1}.[37,40,42,43] The weak interactions involve hydrogen bonding of pyridine nitrogen with a band shift to higher wavenumber (+5−6 cm^{-1}) from 1597 cm^{-1}.[37,44]

FTIR Spectra of NREP Blends: (A) NREP−Zein Blends. In Zein, the broad band of amide I is seen at 1657 cm^{-1} (Figure 2). It corresponds to two populations of carbonyl groups: (1) free and (2) involved in intramolecular associations with NH groups. Similar features for amide bands in poly(ether amide) have been reported.[45]

Polyamides are proton acceptors and form hydrogen bonds with proton donors like carboxylic, hydroxyl, and phenolic groups.[45,46] Zein contains amide groups and acts as a proton acceptor like NREP. Both NREP and Zein exhibit self-association, which needs to be overcome to ensure miscibility. There still exists a possibility of interaction between hydroxyls

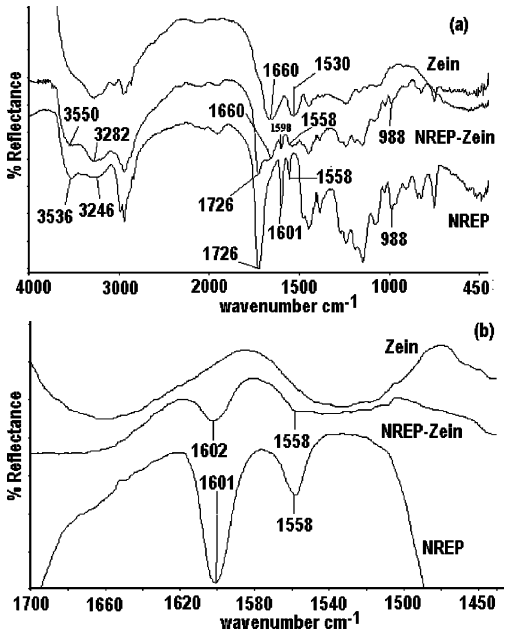

Figure 2. (a) FTIR spectra of NREP−Zein blends. (b) Scale-expanded spectra.

from NREP with the amide carbonyl of Zein, rendering the blends either miscible or partially miscible. The mixing of NREP with Zein resulted in immediate phase separation. The bands for amide I and II of Zein appear unaffected in the NREP−Zein blend (see Figure 2). The frequency for the free hydroxyl of NREP is unaltered in the blend. The pyridine bands at 1601 and 1558 cm^{-1} in NREP are also unaltered. The amide bands are reported to shift as a result of hydrogen bonding.[45,47] However, such changes are not observed, suggesting that the amide groups are not involved in hydrogen bonding with hydroxyls of NREP. It is expected that NREP−Zein blends would exhibit two T_gs owing to partial miscibility or immiscibility.

(B) NREP−EC Blends. The presence of cellulosic hydroxyls in EC enables it to participate in hydrogen bonding. The band for free hydroxyl group in EC is seen at 3485 cm^{-1} (see Figure 3). It does not show a shoulder at lower frequency corresponding to hydrogen-bonded hydroxyls.

NREP can form miscible blends with EC via hydrogen bonding involving hydroxyl−hydroxyl, hydroxyl−carbonyl, and hydroxyl−pyridine nitrogen from EC and NREP (see Scheme 3S in Supporting Information). The film of NREP−EC blend is transparent. The FTIR spectrum of NREP−EC blend shows a fall in intensity for the free hydroxyl group at 3483 cm^{-1} as compared to neat EC. Further it shows the appearance of a shoulder at 3285 cm^{-1} for the hydrogen-bonded hydroxyl, indicating weaker association. Lee et al.[48] reported that hydrogen bonds in polymer blends differ in strength. Strong bands appear at 2800, 2500, and 1800 cm^{-1}, the moderate to intermediate strength bands appear at 3100−2800 cm^{-1}, and a weak structureless broad band appears at 3300 cm^{-1}. This substantiates our findings.

The carbonyl band in NREP−EC blend is seen at 1726 cm^{-1} with a shoulder at 1635 cm^{-1}. This shoulder is more profound in the blend than in neat NREP. This indicates the participation of carbonyl groups of HEMA or MMA from NREP in hydrogen bonding with hydroxyl groups of EC. The bands at 1601 and 1558 cm^{-1} for pyridine group are unaltered in the NREP−EC blend. Thus pyridine nitrogen is not involved in hydrogen bonding (see Figure 3). From the interactions observed above,

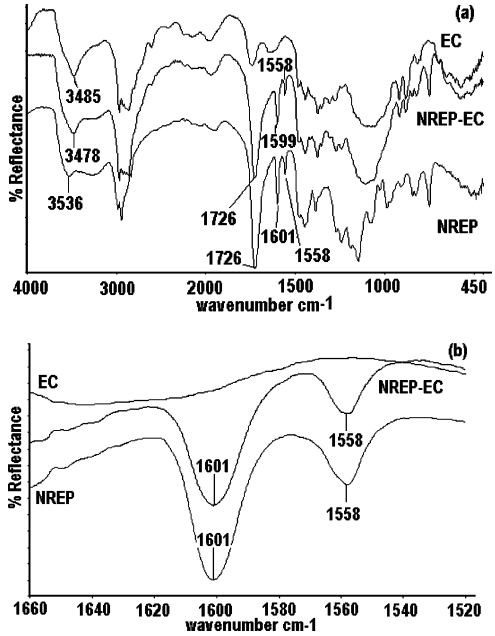

Figure 3. (a) FTIR spectra of NREP−EC blends. (b) Scale-expanded spectra.

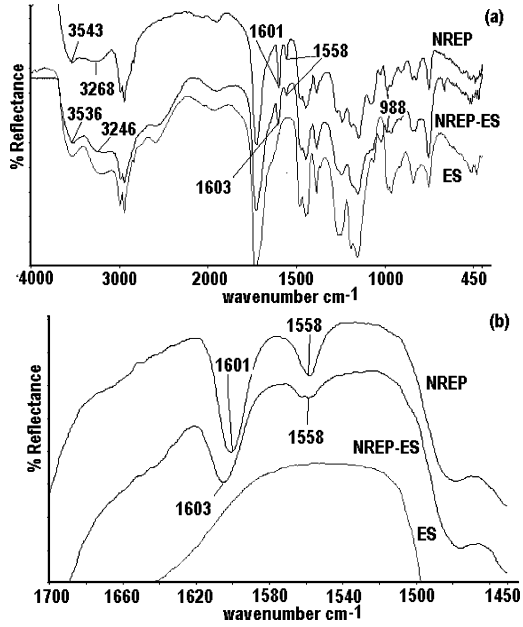

Figure 4. (a) FTIR spectra of NREP−ES blends. (b) Scale-expanded spectra.

NREP−EC may be expected to exhibit a single composition-dependent T_g. However, the extent of interaction in NREP−EC is weak; hence negative deviations from additivity are expected.

(C) NREP−ES Blends. The spectrum of ES in the hydroxyl stretching region shows the presence of free hydroxyl groups (3500−3550 cm^{-1}) and a shoulder at 3200 cm^{-1}. This indicates hydrogen-bonded hydroxyls (Figure 4). The carbonyl stretching region of ES spectrum shows maxima at 1727 cm^{-1} for C═O groups (acid and ester carbonyl) and a shoulder at 1635 cm^{-1}. The presence of a shoulder indicates self-associations in ES, due to hydrogen bonding between the acid hydroxyls (COOH) and carbonyl from the acrylic ester and carboxylic groups. Existence of association between C═O and acid hydroxyls in Eudragit L (EL) was reported in the past,[49] and our findings are similar to these. The salt formation of EL and ES with polybases results in generation of two new bands at 1560 and 1400−1300 cm^{-1}.[21] Blending of polybase NREP with polyacid ES is expected to show changes in the pyridine ring mode, hydroxyl, and carbonyl stretching region. The NREP−ES blend was examined for carboxylate salt formation (see Schemes 4S and 5S in Supporting Information).

Hydroxyl Stretching Region. Both NREP and ES show bands at 3540−3550 cm^{-1} for free hydroxyl groups. A decrease in intensity for this band is seen in the blend. The region 2500−3500 cm^{-1} in NREP−ES blend shows significant band broadening due to hydrogen bonding. Further, the blend shows a band for free hydroxyls at 3536 cm^{-1} with a shoulder at 3268 cm^{-1}. The appearance of this band at 3268 cm^{-1} suggests weaker hydrogen bonding in hydroxyl groups as reported by Lee et al.[48]

Carbonyl Stretching Region. The band for carbonyl in NREP−ES blend is broader than that seen in neat NREP, indicating hydrogen bonding of the NREP carbonyl with hydroxyl of ES. However, the carbonyl band in blend is narrower than that seen in neat ES. This indicates that the self-association between carbonyl and hydroxyl within ES is overcome and the carboxylic hydroxyl now participates in interpolymer association with NREP. This causes liberation of carbonyl from self-association in ES. This is reflected in the spectrum, which shows a maximum at 1726 cm^{-1} and shoulder at 1703 cm^{-1}. Similar results were reported for methacrylic acid and vinylpyridine groups.[48] No new bands were observed in the region of 1560 cm^{-1}, confirming that no carboxylate salt was formed between NREP and ES.

Pyridine Ring Mode. The 1558 cm^{-1} band for pyridine ring in NREP remains unaltered in the NREP−ES blend. The band at 1601 cm^{-1} in neat NREP shifts to 1603 cm^{-1} in the NREP−ES blend. This shift to higher wavenumber indicates participation of pyridine nitrogen in intermolecular hydrogen bonding. Similar shifts (+5−6 cm^{-1}) for hydrogen-bonded pyridine nitrogen in blends of poly(VP) with poly(vinyl acetate-*co*-vinyl alcohol)/poly(HEMA)/poly(monomethyl itaconate) and pentadecylphenol have been reported.[33,36,37,50] The scale-expanded spectrum (Figure 4b) shows that there are no new bands generated in the region 1618−1637 cm^{-1}. Thus protonation of the pyridine group to pyridinium has not occurred. The intermolecular associations in NREP−ES are of weaker magnitude, rendering the polymers miscible without complexation. Hence positive deviations in T_g from weight average are not expected. But the interaction in NREP−ES is stronger than that seen in NREP−EC, so the NREP−ES blends are expected to show slower release of CA than that seen in NREP−EC.

(D) NREP−HPMCP Blends. HPMCP contains cellulosic hydroxyls in addition to acid hydroxyls. The carboxylic groups in HPMCP are attached to the aromatic ring and are therefore more amenable to dissociation due to stabilization effects of the ring. The spectrum of HPMCP shows bands for free hydroxyl groups at 3483 and 3473 cm^{-1} (see Figure 5). The carbonyl band appears at 1725 cm^{-1} for HPMCP and shows a shoulder at lower frequency, indicating self-association. The carbonyl is hydrogen-bonded with acid or cellulosic hydroxyls (see Schemes 6S and 7S in Supporting Information).

Hydroxyl Stretching Region. The NREP−HPMCP blend shows a free hydroxyl band at 3511 cm^{-1} and a slight shoulder at 3297 cm^{-1} (see Figure 5). The neat NREP shows a distinct band for hydrogen-bonded hydroxyls at 3285 cm^{-1}, whereas the NREP−HPMCP blend shows the same at 3297 cm^{-1}. This shift indicates increase in intensity of hydrogen bonding.

Carbonyl Stretching Region. The carbonyl band in the

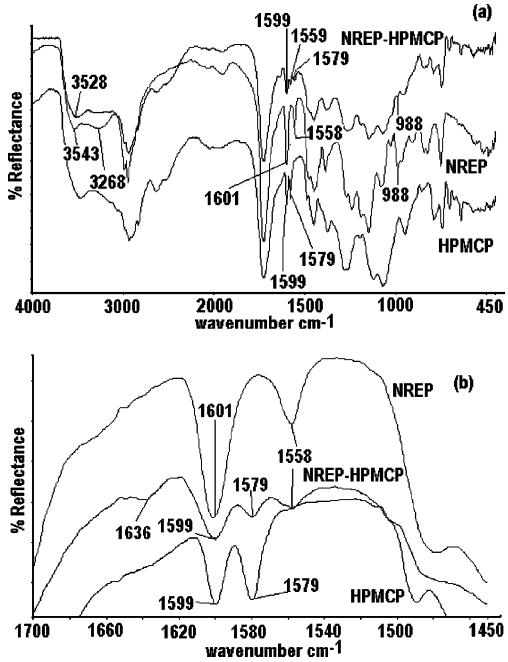

Figure 5. (a) FTIR spectra of NREP−HPMCP blends. (b) Scale-expanded spectra.

NREP−HPMCP blends is narrower than that seen in HPMCP but broader than that in neat NREP. This shows that the self-association in HPMCP between carbonyl group and acid hydroxyls is overcome and the carbonyl group is liberated. The acid hydroxyls in carboxylic groups from HPMCP participate in intermolecular associations with NREP.

Pyridine Ring Mode. HPMCP showed bands at 1599 and 1579 cm^{-1}. The spectrum of NREP−HPMCP in the region 1700−1450 cm^{-1} showed three bands at 1599, 1579, and 1558 cm^{-1} (see Figure 5b). The band for pyridine at 1601 cm^{-1} in NREP is merged with the band at 1599 cm^{-1} of HPMCP. However, the second band at 1579 cm^{-1} for HPMCP and the third band at 1558 cm^{-1} due to the pyridine ring of NREP are resolved. The other band corresponding to pyridine ring at 990 cm^{-1} in NREP appears in the NREP−HPMCP blend at 988 cm^{-1}. Since bands at 1601 and 1599 cm^{-1} in NREP and HPMCP are too close to be resolved, the band at 1558 cm^{-1} for NREP was examined. The scale-expanded spectrum of the NREP−HPMCP blend shows a clear band at 1558 cm^{-1} and slight emergence of a new band at 1636 cm^{-1}. Since the content of pyridine is too low in NREP, the absorption of this band is not evident without scale expansion. The coexistence of the bands at 988 and 1558 cm^{-1} along with the emergence of a weak new band at 1636 cm^{-1} in NREP−HPMCP blend suggests partial conversion of pyridine groups to pyridinium. Partial protonation of pyridine in blends of poly(2VP) with poly(monomethyl itaconate) and poly(ethylene-*co*-methacrylic acid) has been reported in the past.[36,48]

The complete conversion of pyridine to pyridinium would result in complex formation, which we did not observe. The partial conversion observed might be attributed to the presence of (1) a nonionic structural defect in NREP, (2) lower content of pyridine, or (3) low pK_a value of 4VP. It has been reported that blends of poly(4VP) with poly(HEMA) did not result in complexation.[33] The presence of nonionic structural defect in polyacids or polybases restricts complexation with oppositely charged polymer.[29,39,48,51] NREP contains HEMA, which may act as a structural defect, thereby avoiding complex formation between NREP and HPMCP. Complexation between pyridine and phenolic units was inhibited due to lower content of 4VP and the presence of intercalated styrene units.[52] The composition of NREP is shown in Table 1. The lower content of pyridine as compared to carbonyl and hydroxyl groups may also help in inhibition of complexation with polyacids. From the FTIR studies it was concluded that NREP−HPMCP blends exhibited the strongest interaction among all the systems.

Table 2. T_g of Neat Polymers

	T_g (°C)		
polymer	observed	reported	refs
ES	172.8	163,171	21, 59
EC	135.8	133.4, 125	60, 61
NREP	121.2		
HPMCP	137	~150	62
Zein	164.4	156,164	53, 63

Table 3. Parameters Derived by Equation 3

blend	$K = T_{g1}/T_{g2}$	K_1	K_2	$K_1 - K_2$
NREP−EC	0.89	−0.62	0.59	−1.14
NREP−ES	0.70	−0.08	0.47	−0.55
NREP−HPMCP	0.88	0.01	1.78	−1.77

Thermal Analysis. The T_g values of neat polymers observed are shown in Table 2 and these are in good agreement with those reported in literature. The values of fitting parameters are given in Table 3.

(A) NREP−Zein Blends. The films cast from NREP−Zein showed distinct transparent and opaque regions indicating phase separation. This was reflected in thermal analysis with appearance of two T_gs for all compositions as seen in Figure 6a. The lower T_g corresponds to the NREP-rich phase and the higher T_g to Zein-rich phase. The T_g versus composition plots (Figure 6b) did not show a consistent composition dependence. T_g for Zein shifted to a higher value (169−170 °C) from 164.4 °C, while for the NREP-rich phase, the T_g shifted below 121.2 °C

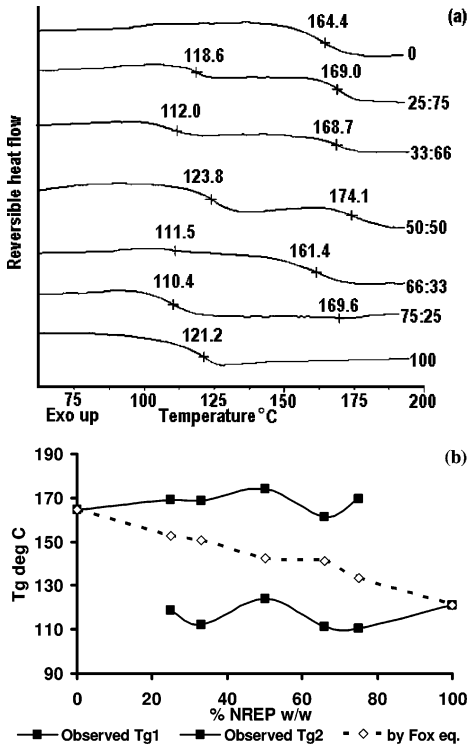

Figure 6. Thermal analysis of NREP−Zein blends: (a) thermograms; (b) T_g vs composition plot.

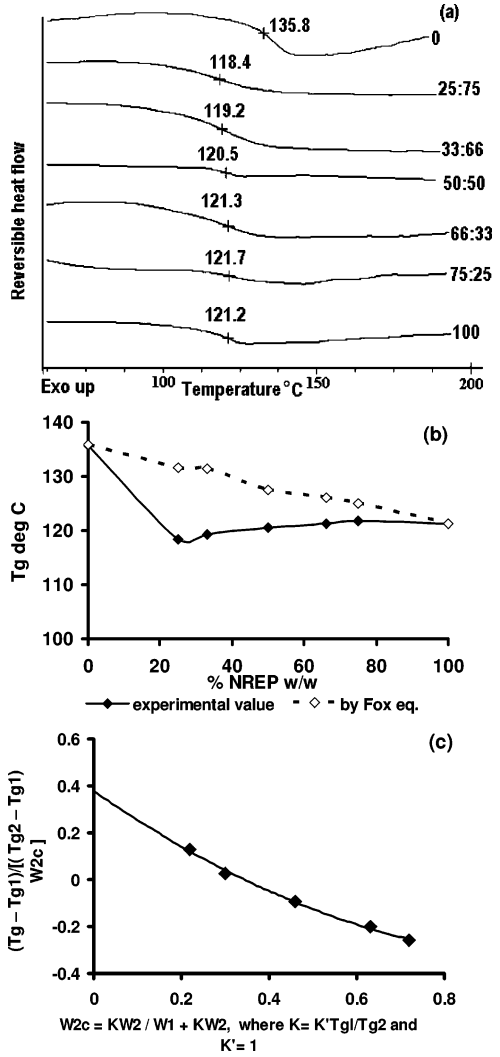

Figure 7. Thermal analysis of NREP−EC blends: (a) thermograms; (b) T_g vs composition plot; (c) T_g composition data as per eq 3.

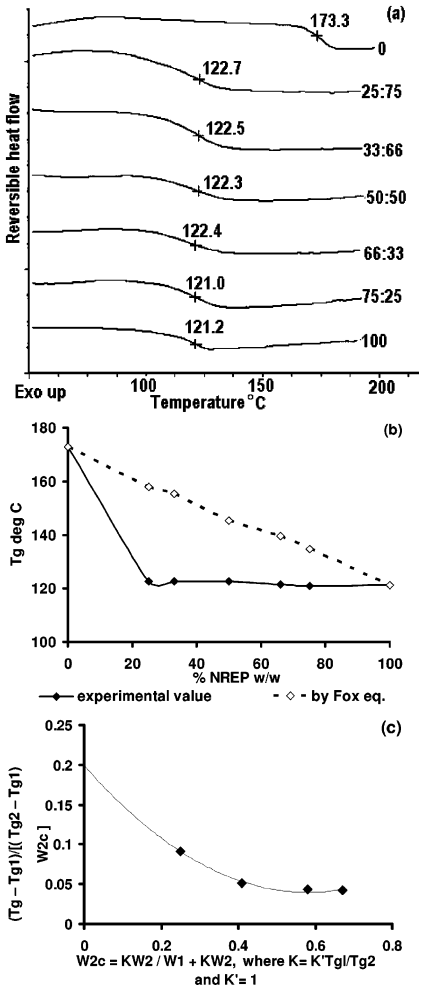

Figure 8. Thermal analysis of NREP−ES blends: (a) thermograms; (b) T_g vs composition plot; (c) T_g composition data as per eq 3.

(Figure 6b). The shift in T_g of amorphous Zein films from 165 °C to higher value (∼170 °C), due to conformational change from random coil to α and β form, leading to partial crystallization, is reported.[53] The presence of moisture cleaves the intra- and intermolecular bonding in Zein, contributing to these effects. The fall in T_g of NREP could be due to the presence of Zein molecules in between the polymer chains. Since both Zein and NREP are proton-accepting polymers, they do not interact, which results in immiscibility. Hence, to attain the sustained gastric release of CA, large amounts of Zein would be required along with NREP.

(B) NREP−EC Blends. The NREP−EC blends showed a single T_g at all compositions (Figure 7a). The experimentally obtained T_g values showed large negative deviations from the values calculated by eq 1. T_gs for all blend compositions were within 3 °C and did not vary with composition (Figure 7b).

The extent of interactions was quantified by fitting the data in eq 3. The values of parameters K_1 and K_2 obtained were −0.62 and 0.59, respectively (see Figure 7c and Table 3). The negative deviation from additivity reflects weak intermolecular interactions between blend components and is reflected in $K_1 < 0$. EC is nonionic; hence, weak interactions with polybase NREP were expected. NREP and EC chains undergo conformational redistribution to establish hetero contacts responsible for miscibility, which is reflected in K_2 (0.59) > 0. This conformational redistribution leads to change in entropy with increase in free volume. This results in a fall in T_g of the blend as compared to the predictions based on volume additivity. The parameter K_2 is the difference of effects of redistributions predominantly in environment of components 1 and 2. $K_2 > 0$ reflects more conformational changes occurring in NREP than in EC, which is expected due to the bulky/rigid structure of EC as compared to NREP.

(C) NREP−ES Blends. Normally interactions between polyacids and polybases result in charge transfer with polyelectrolyte salt formation. The T_g versus composition curves for such systems result in large positive deviations from additivity.[29] The NREP−ES blends formed clear films at all compositions. The blends showed a single T_g at all compositions, indicating miscibility (Figure 8a). However, the experimentally obtained T_g values showed large negative deviation from the weight average T_gs (Figure 8b). The T_g values of NREP−ES blends do not exhibit variation with composition and lie within a narrow range of 121−123 °C. The K_1 and K_2 values obtained for NREP−ES blends are −0.08 and 0.47, respectively (Figure 8c and Table 3). The value $K_1 < 0$ was expected since negative deviations for blend T_gs were observed from volume additivity. The lower charge densities on NREP and ES contribute to conformational redistributions, to establish the hetero contact for favorable energetic interactions. The strong self-association between hydroxyl of HEMA with pyridine nitrogen in NREP is overcome to establish the hetero contact with acid hydroxyl of ES. The large negative deviations from additivity can be explained on the basis of these conformational changes con-

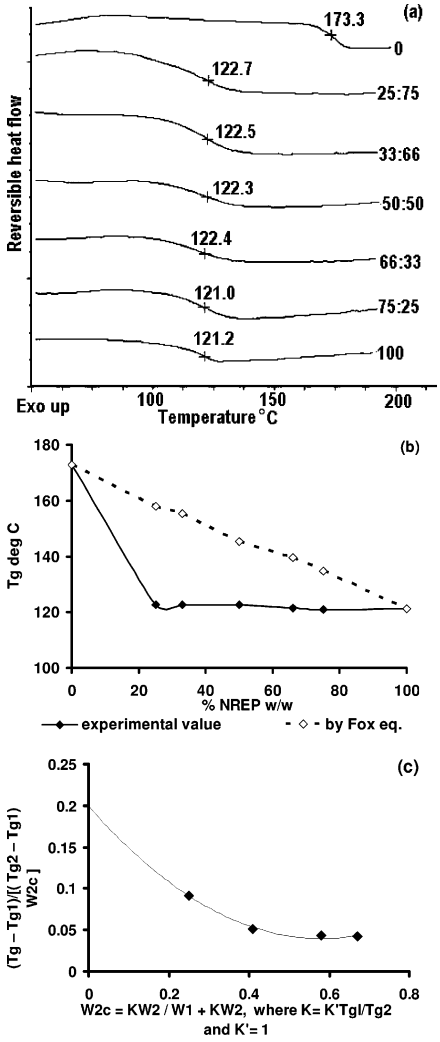

Figure 9. Thermal analysis of NREP−HPMCP blends: (a) thermograms; (b) T_g vs composition plot; (c) T_g composition data as per eq 3.

tributed by both components in NREP−ES blends. Hence the value of K_1 (−0.08) in NREP−ES blend is greater than for NREP−EC (−0.62).

(D) NREP−HPMCP Blends. NREP at all compositions formed a clear film with HPMCP. The blends showed a single composition-dependent T_g, which increased with increase in HPMCP content, indicating miscibility (Figure 9a). As seen in earlier cases, the NREP−HPMCP blends showed negative deviations from the weight-average T_g values, reflecting weaker interactions between these polymers (Figure 9b). Data treatment with eq 3 yielded $K_1 = 0.01$ and $K_2 = 1.78$ (see Figure 9c).

The value of K_1 (0.01) was larger for NREP−HPMCP than that observed for NREP−ES (−0.08), indicating stronger interaction. The FTIR analysis also supports this, since partial protonation of pyridine to pyridinium in NREP−HPMCP blends was seen. The positive value of K_1 reflected the favorable energetic interactions by hetero contact formation in NREP and HPMCP. However, this did not result in complete charge transfer. There was no stiffening of donor chain; the deviations of blend T_gs from predictions of eq 1 are still negative. For this system too, the value of K_2 reflected large contributions toward the blend T_g, arising from conformational redistributions in NREP and HPMCP chains, to establish the hetero contact. The positive value of K_2 (1.78) reflected the predominant contribution from NREP in conformational changes. This was expected as HPMCP has a bulky structure.

Table 4. CA Formulations Based on NREP and Its Blends with Polymers

formulation[a]	NREP	other polymers[b]	total polymer[c]
F1	1200		1200
F2	600		600
F3	300	Zein (600)	900
F4	300	Zein (150), EC (25)	475
F5	300	EC (45)	345
F6	300	EC (60)	360
F7	300	EC (100)	400
F8	200	ES (100)	300
F9	300	HPMCP (50)	350
F10	200	HPMCP (200)	400
F11	200	HPMCP (300)	500
F12	300	HPMCP (25), EC (15)	340
F13	300	HPMCP (25), ES (15)	340

[a] Different formulations containing 600 mg of CA. [b] Values in parentheses are weight fractions of other polymer in milligrams. [c] Total polymer content in formulation.

The values of parameters K_1 and K_2 were larger for NREP−HPMCP than those seen in NREP−ES and NREP−EC (see Table 3). The structural symmetry due to the presence of cellulose ring and aromatic ring in HPMCP and NREP, respectively, help in establishing better hetero contact than that seen in NREP−ES. The probability of interaction is influenced by favorable structural symmetry factors in polyacceptor/polydonor, which contribute to increased formation of hetero contacts.[23,24,54]

CA Release from Microparticles. The enteric polymers ES and HPMCP prevent drug release at acidic pH. The immediate release of drugs from reverse enteric polymer at acidic pH is well-known. The effect of blending enteric polymers with NREP is discussed below. An advantage of using NREP as the cationic polymer along with enteric polymers was that a hydrophobic coherent film could be formed. The hydrophobic nature of the film coating is particularly useful for CA, as it tends to gel in presence of moisture with loss of bioavailability. The FTIR studies of NREP blends with all polymers showed the presence of free pyridine groups. These blends were expected to show pH-dependent behavior at acidic pH as the free pyridine is available for protonation. These blends were ideal for CA, which is absorbed primarily in upper gastric region. Another advantage of using these hydrophobic blends is that the coated microparticles can be used in the pediatric formulations such as granules for reconstitution. These coatings would provide sustained release along with taste masking. The different compositions used for encapsulating CA are shown in Table 4.

The dissolution of CA from NREP-coated microparticles is shown in Figure 10. NREP releases 80% of CA in 30 min and 90% in 60 min. CA release from NREP-coated microparticles occurs by dissolution of NREP resulting from protonation of pyridine nitrogen. Both formulations (F1 and F2) showed a very rapid release at pH 1.2. It has been reported in the past that once the solvent has diffused into the glassy polymer reaching a critical concentration, the polymer chain disentanglement dominates and the polymer begins to dissolve.[55] Various models for polymer dissolution have been proposed.[56] The dissolution of glassy polymer involves three steps. In the first step, solvent molecules diffuse into the polymer matrix. This is followed by the relaxation of polymer chains initiated by the penetration of the solvent molecules and formation of a swollen gel. In the final step, polymer chains diffuse out from the gel into the solvent reservoir. In the present investigation CA is dispersed

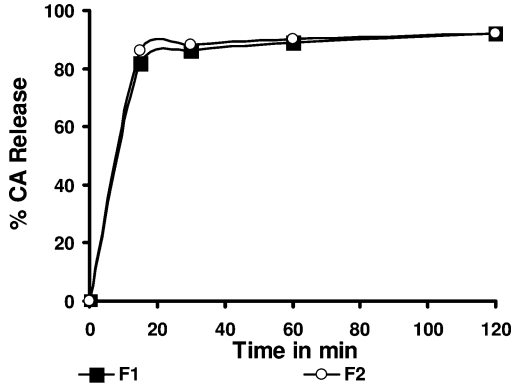

Figure 10. CA release from NREP microparticles.

in the matrix of NREP and the dissolution of NREP causes the release of CA into surrounding acidic buffer medium.

The content of NREP was high in all the polymer blend formulations (F3−F13) as seen from Table 4. So it was expected that CA would be released immediately due to dissolution of NREP. However, the blending of NREP with Zein, EC, ES, and HPMCP resulted in sustained release of CA, due to the polymer−polymer interactions. The release rate decreased as K_1 increased. The interactions of NREP with these polymers resulted in slow progress of the buffer in the glassy core, causing the delay in release. The ionization of free pyridine in blends results in rapid penetration of the acidic buffer initially, resulting in swelling and dissolution of polymer. The desorption of dissolved NREP is seen as pores in the SEM images (Figures 11−14). In most cases, as the sharp penetration of solvent progresses it separates the glassy core from the swollen rubbery phase. The magnitude of polymer relaxation is dependent on relative rate of solvent penetration, resulting in either Fickian or non-Fickian behavior.[57] We observed that as the extent of interaction between NREP blends increased, the rate of buffer penetration slowed. This is reflected in the release attaining Fickian pattern for NREP−HPMCP blends where the extent of interaction was highest as seen from the highest K_1 value obtained for this blend.

Table 4 shows the formulations based on NREP and its blends. The release exponents are summarized in Table 5. In the present system the CA release has to be completed in the gastric region before transit to the small intestine, and hence a rapid release followed by slow release for 3−4 h is preferred. In some cases burst release is also favored.[58] The release profiles from polymer blends are discussed below in detail and explained on the basis of predictions made from MDSC and FTIR analysis.

NREP−Zein-Based CA Microparticles. The MDSC and FTIR analysis had shown that NREP and Zein were immiscible,

Table 5. Kinetic Parameters Based on Equation 4

formulation[a]	kinetic parameter (k)	release exponent (n)	correlation coefficient
F3	51.2	0.20	0.98
F4	58.8	0.26	0.97
F5	66.0	0.24	0.98
F6	66.0	0.23	0.91
F7	60.2	0.18	0.93
F8	55.0	0.20	0.96
F9	60.0	0.22	0.97
F10	46.7	0.42	0.99
F11	35.1	0.46	0.99

[a] Different formulations containing 600 mg of CA.

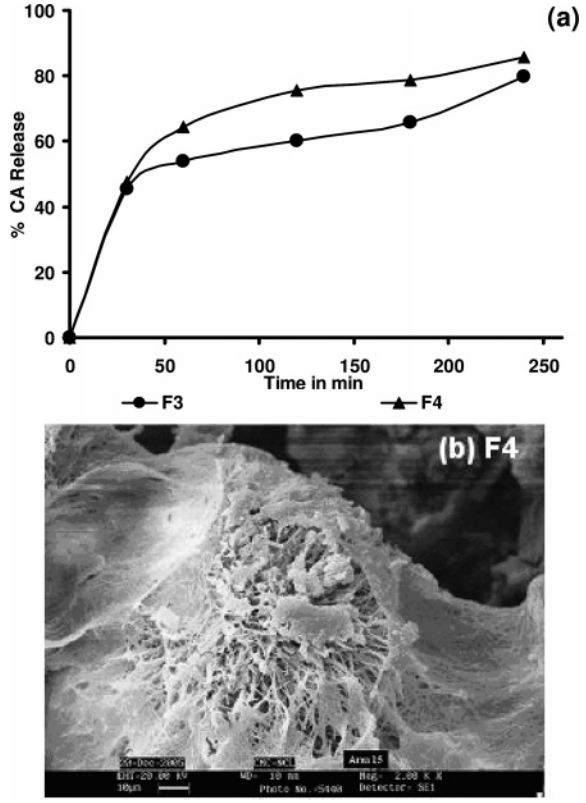

Figure 11. (a) CA release from NREP−Zein blends. (b) SEM for microparticles (F4).

so it was expected that formulations based on NREP−Zein would exhibit rapid initial release due to dissolution of NREP at acidic pH. Hence higher content of Zein was used in formulation F3, to sustain CA release at gastric pH. F3 released 45%, 54%, 60%, 65%, and 80% of CA in 30, 60, 120, 180, and 240 min, respectively (Figure 11). CA release for 4 h from F3 was found to be desirable; however, the total amount of polymer required for attaining the release pattern was very high (900 mg). The evaluation of the extent of interaction between polymers by eq 3 provides a measure to decide the blend composition in formulations. For polymers that exhibit better interactions, lower amount of polymer in blends can achieve the same release profile.

From the FTIR and thermal analysis, it was found that EC was miscible with NREP and exhibited better interaction than that exhibited by Zein. Formulation F4, based on NREP, Zein, and EC blends, was therefore designed. The total polymer content in F4 was 475 mg as compared to 900 mg in F3. The initial CA release from F3 and F4 is comparable in spite of reduction in total polymer content, which is attributed to stronger interaction in NREP−EC than in NREP−Zein (see Figure 11). The lowering of Zein content in F4 resulted in a slight increase of CA release at the end of 4 h in comparison with that seen for F3. The SEM for F4 microparticles (Figure 11b) shows porosity generated due to dissolution of NREP. The release data on treatment with eq 4 showed that the value of k was higher, indicative of burst release. This further validated the conclusions drawn from the MDSC and FTIR studies for miscibility of NREP with Zein. The release of CA was sustained up to 4 h in F3 and F4 compared to the rapid release from F1 and F2.

NREP−EC-Based CA Microparticles. The MDSC and FTIR analysis showed that NREP−EC blend is miscible but it exhibits weak interactions, which can be overcome by the interaction between the acidic buffer and NREP. Hence a burst

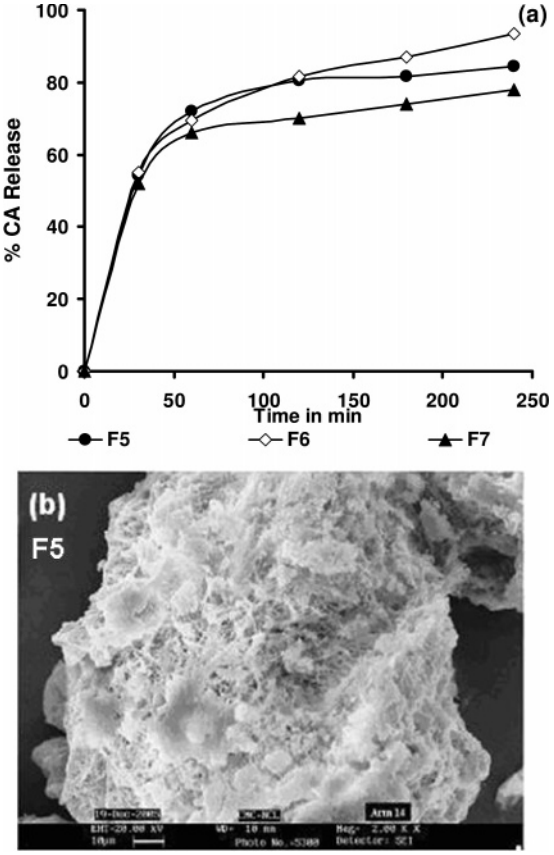

Figure 12. (a) CA release from NREP−EC blends. (b) SEM for microparticles (F5).

followed by slow release is expected. CA release for F5 and F6 based on NREP−EC is shown in Figure 12a. The rapid release of CA from F5 and F6 occurs from the pores generated by dissolution of NREP, as seen from the SEM images (Figure 12b). The higher value of kinetic parameter for F5 and F6 (k = 66, each) further substantiates this. The CA release is slowed thereafter due to the interactions between NREP and EC. With a slight increase in concentration of EC in F6, CA release was slowed after 2 h (Figure 12a).

The weak interaction between NREP and EC makes it difficult to control initial rapid release. Since the extent of interaction is weak, the free pyridine from NREP will protonate and cause initial rapid release in acidic pH. To verify this, dissolution of CA from another formulation (F7) with a higher content of EC (100 mg) was investigated. The initial release from F7 was comparable to that from F5 and F6; however, retardation in CA release after 1 h was observed. Any further increase in EC content to lower the initial CA release would not be useful, and furthermore, it would result in retardation of release after 1 h. Hence, formulations containing still higher loading of EC were not attempted. Instead, formulations with polymers exhibiting better interaction than EC with NREP were investigated.

NREP−ES-Based CA Microparticles. CA release from F8 based on NREP−ES is shown in Figure 13a. The greater interaction exhibited by NREP−ES than NREP−EC enabled us to retard CA release from F8 compared with that seen for F5 and F6. Further, the total polymer loading in F8 is 300 mg, as compared to 345 and 360 mg in F5 and F6, respectively. Also, in comparison to the formulations based on Zein (F3 and F4), the NREP−ES-based formulation was able to retard the CA release at lower polymer loading. This is attributed to better interaction in NREP−ES than in NREP−EC/Zein.

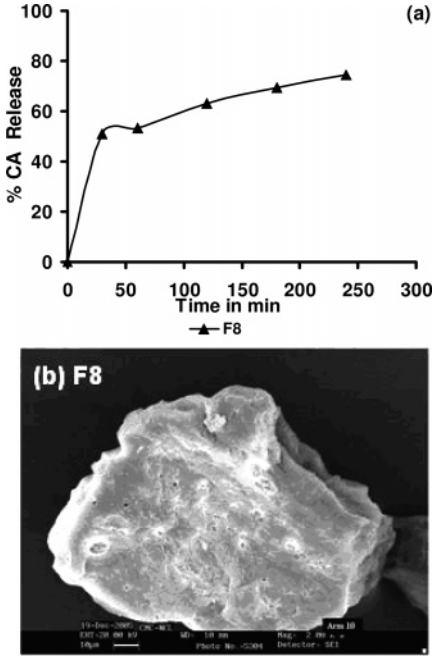

Figure 13. (a) CA release from NREP−ES blends. (b) SEM for microparticles (F8).

The values of parameters K_1 and K_2 for NREP−ES are higher than those for NREP−EC. The FTIR spectrum of NREP−ES showed a shift for the pyridine group from 1601 to 1603 cm^{-1}, indicating participation of pyridine nitrogen in hydrogen bonding with ES. Such behavior was not seen in the FTIR spectrum of NREP−EC. ES exhibits better miscibility with NREP than EC. Hence the initial release from NREP−ES blend was expected to be lower than that observed for NREP−EC system and this has been confirmed. The value of parameter K_1 (−0.08) was not very high for NREP−ES blends. Hence the initial burst release would be observed even on altering the blend compositions at acidic pH. The hydrogen bonding between NREP−ES is weak without conversion of pyridine to pyridinium units. These free pyridine nitrogens protonate in acidic buffer responsible for the burst release seen for F8.

The data treatment by eq 4 showed higher value of k for F8 (55.0), and the SEM image (Figure 13b) for microparticles after dissolution further substantiates this. CA release is slowed thereafter, reaching 74% at the end of 4 h. Formulations with increase in ES content to control burst effect would not be useful. Similar conclusions were reached in the case of NREP−EC blends. Further lowering of ES content would result in increased initial CA release, which was not desired. Hence such formulations were not attempted. There is a marked difference in the morphology of NREP−ES-based microparticles as compared to those based on NREP−Zein and NREP−EC. The NREP−ES structure is less porous as compared to NREP−Zein and NREP−EC, as seen from Figures 11−13.

NREP−HPMCP-Based CA Microparticles. HPMCP exhibited the strongest interaction with NREP among all the polymers investigated. The FTIR analysis showed that pyridine nitrogen in NREP is partially converted to pyridinium units by HPMCP. This indicates that all the pyridine nitrogen are not free for protonation by acidic buffer; hence the initial rapid release would be suppressed. Hence incorporation of lower quantities of HPMCP would retard CA release substantially. Formulation F9 with 50 mg of HPMCP and 300 mg of NREP was considered for sustaining CA release.

F9 releases 53%, 65%, 76%, and 87% of CA after 30, 60, 120, and 240 min, respectively (Figure 14a). Due to stronger

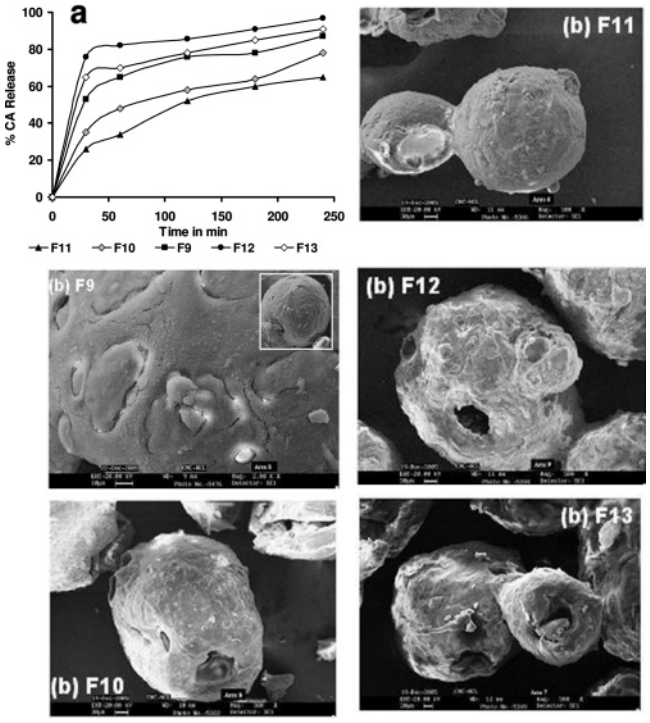

Figure 14. (a) CA release from NREP−HPMCP blends. (b) SEM for microparticles (F9−F13).

interaction between NREP and HPMCP, even a small amount of HPMCP (50 mg) blended with large amounts of NREP (300 mg) was effective in sustaining CA release up to 4 h. The release from F9 was retarded as compared to earlier formulations and this can be attributed to the highest interaction exhibited by NREP−HPMCP compared with the other blends investigated. The value of the kinetic parameter derived from eq 4 was $k = 60$, indicating initial burst release. The FTIR analysis showed that only partial pyridine is converted to pyridinium, and the partially free pyridine is responsible for initial burst release. The SEM of microparticles is shown in Figure 14b. The surface morphology of NREP−HPMCP microparticles (F9) shows less porosity compared to earlier formulations (F4, F5, and F8).

To validate the earlier assumption that extent of interaction affects the release pattern from the polymer blends, two formulations (F10 and F11) with higher HPMCP content were formulated. As the content of HPMCP increased, the amount of free pyridine in NREP−HPMCP blends would be lowered due to formation of pyridinium units. The dissolution of NREP in acidic buffer would be retarded, resulting in lower initial release. The T_g versus composition plot showed that at 50:50 (w/w %) NREP−HPMCP, the experimental T_g value was close to weight-average T_g. Since NREP−HPMCP exhibits good miscibility at this composition, it was selected for formulation F10. Both F10 and F11 showed retardation in release as compared to F9 (see Figure 14a). F10, containing 200 mg of HPMCP, showed faster release than F11, containing 300 mg of HPMCP. The release data for F10 and F11 on treatment with eq 4 showed diffusion-controlled release with $n = 0.42$ and 0.46, respectively ($k = 46$ and 35.1, respectively). Due to better miscibility of NREP−HPMCP at above-mentioned compositions, a burst release is not observed as seen in formulations based on Zein, EC, and ES. The SEM images (Figure 14b, F10 and F11) show some part of NREP dissolved, creating craters. However the particle does not show an open porous structure. Thus CA is released from the matrix by diffusion. CA release was significantly sustained in F11, with 60% being released after 4 h. Since CA is absorbed in the upper gastric region, this release pattern would not be desirable. However, such sustained release would be desirable for drugs absorbed throughout the gastric tract. These results will be discussed later.

To validate whether low extent of interaction results in rapid release from blends, a third component with lower interaction than HPMCP with NREP was introduced. Two formulations (F12 and F13) with EC and ES, respectively, were formulated. CA release was faster from F12 when compared with F9, F10, and F11 (see Figure 14a). Formulation F12 released 76% of CA in 30 min and 97% after 4 h. From Table 3 it can be seen that K_1 for NREP−EC is lower than for NREP−HPMCP, which accounts for higher CA release from F12. The SEM for formulation F12 (Figure 14b) shows open porous structure generated as a result of dissolution of CA and NREP. The release of CA from F13 was slightly retarded as compared to F12 (see Figure 14a). The extent of interaction contributes to the observed release pattern, as the K_1 value for ES was greater than that obtained for EC. SEM for F13 shows formation of pores contributing to initial burst release. When polymers constituting the blend exhibit weak interaction, the release pattern shows a significant burst followed by sustained release. When the interactions are strong, the burst is suppressed and the release is sustained. The extent of initial burst release and the period of sustained release can thus be manipulated by the judicious choice of polymer constituents as well as the polymer compositions. Incorporation of HPMCP, which has a relatively higher extent of interaction with NREP, helps to sustain CA release at the lowest possible loading.

Conclusions

The release rates of the drugs from the excipient blends can be systematically varied only if the blends are miscible. The understanding of interactions between the constituents of polymer blends gained from FTIR studies and thermal analysis has been exploited to tailor sustained release of CA at gastric pH. NREP is immiscible with Zein and completely miscible with EC, ES, and HPMCP at all compositions. The miscibility is governed by the degree of interactions between the blend constituents, which in turn affects the release pattern. The T_g data analyzed in terms of the Schneider equation shows that the order of interaction of these polymers with NREP is EC < ES < HPMCP. The parameters of the Schneider equation provide a guideline for the choice of the blend constituents. Blends containing EC, which exhibits weak interaction with NREP, show fast release of CA due to dissolution of NREP. Blends of HPMCP, which shows the highest interaction with NREP, can be optimized to yield diffusion-controlled release. The blends reported here can be further tailored to attain sustained release in the intestinal region, depending upon the pharmacokinetic needs of the drug. Thus the miscibility of reverse enteric and enteric polymers without complexation provides a new set of blends that can be optimized to attain a variety of release patterns from film coating.

Acknowledgment. A.R.M. thanks CSIR, New Delhi, India, for financial support.

Supporting Information Available. Structures of polymers and schematic representation of interactions within polymer and their blends. This material is available free of charge via the Internet at http://pubs.acs.org.

References and Notes

(1) Lecomte, F.; Siepmann, J.; Walther, M.; MacRae, R. J.; Bodmeier, R. *J. Controlled Release* **2003**, *89*, 457−471.

(2) Liu, J.; Lin, S.; Li, L.; Liu, E. *Int. J. Pharm.* **2005**, *298*, 117−125.
(3) Ceftin Prescription Information. In *Physicians' Desk Reference*; Thomson Healthcare: Montvale, NJ, 2003; 1918−1922.
(4) Finn, A.; Straughn, A.; Meyer, M.; Chubb, J. *Biopharm. Drug Disposit.* **1987**, *8*, 519−526.
(5) Campbell, C. J.; Chantrell, L. J.; Eastmond, R. *Biochem. Pharmacol.* **1987**, *36*, 2317−2324.
(6) Dantzig, A. H.; Dale, C.; Duckworth, L.; Tabas, B. *Biochim. Biophys. Acta* **1994**, *1191*, 7−13.
(7) Lorenzo-Lamosa, M. L.; Cuna, M.; Vila-Jato, J. L.; Torres, D.; Alonso, M. J. *J. Microencapsulation* **1997**, *14*, 607−616.
(8) Cuna, M.; Lorenzo-Lamosa, M. L.; Vila- Jato, J.; Torres, D.; Alonso, M. J. *Drug Dev. Ind. Pharm.* **1997**, *23*, 259−265.
(9) Deutsch, D. S.; Anwar, J. U.S. Patent 4,897,270, January 30, 1990.
(10) Robson, H.; Craig, D.; Deutsch, D. *Int. J. Pharm.* **1999**, *190*, 183−192.
(11) Menjoge, A. R. Ph.D. Thesis, National Chemical Laboratory, Pune, India, 2006.
(12) Nyamweya, N.; Hoag, S. W. *Pharm. Res.* **2000**, *17*, 625−631.
(13) Kanis, L. A.; Viel, F. C.; Crespo, J. S.; Bertolino, J. R.; Pires, A. T. N.; Soldi, V. *Polymer* **2000**, *41*, 3303−3309.
(14) Mayo-Pedrosa, M.; Alvarez-Lorenzo, C.; Concheiro, A. *J. Therm. Anal. Calorim.* **2004**, *77*, 681−693.
(15) Menjoge, A. R.; Kulkarni, M. G. U.S. Pat. Appl. 2005281874 A1, 2005.
(16) Kulkarni, M. G.; Menjoge, A. R. U.S. Pat. Appl. 20050137372 A1, 2005.
(17) Kulkarni, M. G.; Menjoge, A. R. U.S. Pat. Appl. 20050136114 A1, 2005.
(18) Duodu, K. G.; Tang, H.; Grant, A.; Wellner, N.; Belton, P. S.; Taylor, J. R. N. *J. Cereal Sci.* **2001**, *33*, 261−269.
(19) Bugay, D. E.; Findlay, W. P. *Pharmaceutical excipients: Characterization by IR, Raman, and NMR spectroscopy*; Marcel Dekker: New York, 1999.
(20) Suthar, V.; Pratap, A.; Raval, H. *Bull. Mater. Sci.* **2000**, *23*, 215−219.
(21) Cilurzo, F.; Minghetti, P.; Selmin, F.; Casiraghi, A.; Montanari, L. *J. Controlled Release* **2003**, *88*, 43−53.
(22) Schneider, H. A. Glass Transition (Theoretical Aspects). In *The Polymeric Materials Encyclopedia;* CRC Press, Inc: Boca Raton, FL, 1996.
(23) Schneider, H. A. *Polymer* **1989**, *30*, 771−779.
(24) Schneider, H. A. *J. Res. Natl. Inst. Stand. Technol.* **1997**, *102*, 229−248.
(25) Brekner, M. J.; Schneider, H. A.; Cantow, H. J. *Makromol. Chem.* **1988**, *189*, 2085−2097.
(26) Ritger, P. L.; Peppas, N. A. *J. Controlled Release* **1987**, *5*, 23−36.
(27) Roy, D. S.; Rohera, B. D. *Eur. J. Pharm. Sci.* **2002**, *16*, 193−199.
(28) Jo, W. H.; Cruz, C. A; Paul, D. R. *J. Polym. Sci. Part B: Polym. Phys.* **1989**, *27*, 1057−1076.
(29) Jiang, M.; Li, M.; Xiang, M.; Zhou, H. *Adv. Polym. Sci.* **1999**, *146*, 121−196.
(30) Utracki, L. A. *Polymer alloys and blends, thermodynamics and rheology;* Hanser Publishers/Oxford University Press: New York, 1990.
(31) Moustafine, R. I.; Kabanovaa, T. V.; Kemenovab, V. A.; Van den Mooterc, G. *J. Controlled Release* **2005**, *103*, 191−198.
(32) Moustafine, R. I.; Kemenovab, V. A.; Van den Mooterc, G. *Int. J. Pharm.* **2005**, *294*, 113−120.
(33) Cesteros, L. C.; Meaurio, E.; Katime, I. *Macromolecules* **1993**, *26*, 2323−2330.
(34) Torikai, A.; Hiraga, S.; Fueki, K. *Polym. Degrad. Stab.* **1992**, *37*, 73−76.
(35) Rao, V.; Ashokan, P. V.; Shridhar, M. H. *Mater. Sci. Eng. A* **2000**, *281*, 213−220.
(36) Cesteros, L. C.; Velada, J. L.; Katime, L. *Polymer* **1995**, *36*, 3183−3189.
(37) Ruokolainen, J.; Brinke, G.; Ikkala, O. *Macromolecules* **1996**, *29*, 3409−3415.
(38) Ikkala, O.; Ruokolainen, J.; Torkkeli, M.; Tanner, J.; Serimaa, R.; Brinke, G. *Colloids Surf., A: Physicochem. Eng. Aspects* **1999**, *147*, 241−248.
(39) Iliopoulos, I.; Audebert, R. *Eur. Polym. J.* **1988**, *24*, 171−175.
(40) Pan, Y.; Xue, F. *Eur. Polym. J.* **2001**, *37*, 247−249.
(41) Yarapathi, R. V.; Reddy, S. M.; Tammishetti, S. *React. Funct. Polym.* **2005**, *64*, 157−161.
(42) Goh, S. H.; Lee, S. Y.; Zhou, X.; Tan, K. L. *Macromolecules* **1998**, *31*, 4260−4264.
(43) Kosonen, H.; Valkama, S.; Hartikainen, J.; Eerikalinen, H.; Torkkeli, M.; Jokela, K.; Serimaa, R.; Sundholm, F.; Brinke, G.; Ikkala, O. *Macromolecules* **2002**, *35*, 10149−10154.
(44) Harnish, B.; Robinson, J. T.; Pei, Z.; Ramstrom, O.; Yan, M. *Chem. Mater.* **2005**, *17*, 4092−4096.
(45) Katime, A.; Iturbe, C. C. Hydrogen-bonded blends. In *The Polymeric Materials Encyclopedia*; CRC Press: Boca Raton, FL, 1996.
(46) Mayo-Pedrosa, M.; Alvarez-Lorenzo, C.; Concheiro, A. *J. Therm. Anal. Calorim.* **2004**, *77*, 681−693.
(47) Chen, J. K.; Kuo, S. W.; Kao, H. C.; Chang, F. C. *Polymer* **2005**, *46*, 2354−2364.
(48) Lee, J. Y.; Painter, P. C.; Coleman, M. M. *Macromolecules* **1988**, *21*, 954−960.
(49) Lin, S. Y.; Liao, C. M.; Hsiue, G. H.; Liang, R. C. *Thermochim. Acta* **1995**, *245*, 153−166.
(50) Cesteros, L. C.; Isasi, J. R.; Katime, I. *Macromolecules* **1993**, *26*, 7256−7262.
(51) Krupers, M. J.; Van Der Gaag, F. J.; Feijent, J. *Eur. Polym. J.* **1996**, *32*, 785−790.
(52) Meftahi, M. V.; Frechet, J. M. J. *Polymer* **1988**, *29*, 477−482.
(53) Macoshi, J.; Nakamura, S.; Murakami, K. *J. Appl. Polym. Sci.* **1992**, *45*, 2043−2048.
(54) Schneider, H. A. *Polym. Bull.* **1998**, *40*, 321−328.
(55) Narasimhan, B.; Peppas, N. A. *Macromolecules* **1996**, *29*, 3283−3291.
(56) Pekcan, O.; Ugur, S.; Yllmaz, Y. *Polymer* **1997**, *38*, 2183−2189.
(57) Lee, P. I.; Kim, C. J. *J. Membr. Sci.* **1992**, *65*, 77−92.
(58) Huang, X.; Brazel, C. S. *J. Controlled Release* **2001**, *73*, 121−136.
(59) Lin, S. Y.; Yu, H. L. *J. Polym. Sci., Part A: Polym. Chem.* **1999**, *37*, 2061−2067.
(60) Rowe, R. C. Materials used in the film coating of oral dosage forms. In *Materials used in Pharmaceutical Formulation*; Florence, A. T., Ed.; Blackwell: Oxford, U.K., 1984; pp 2−34.
(61) Pearnchob, N.; Bodmeier, R. *Eur. J. Pharm. Biopharm.* **2003**, *56*, 363−369.
(62) Sertsou, G.; Butler, J.; Scott, A.; Hempenstall, J.; Rades, T. *Int. J. Pharm.* **2002**, *245*, 99−108.
(63) Shukla, R.; Cheryan, M. *Ind. Crops Prod.* **2001**, *13*, 171−192.

BM060540+